Industrial and Domestic Waste Management

Research Article
Volume 4(2), 2024, 71–83
https://doi.org/10.53623/idwm.v4i2.473

Effect of Different Sizes and Heights on the Removal Efficiency of Composite Clay Filter for Gold Mine Site Wastewater Remediation

Abass Adekunle Olatunji[12]*, Ayanniyi Mufutau Ayanshola[3], Mary Adejoke Ajala[4], Ebelechukwu Erhuanga[5]

[1]Department of Civil Engineering, University of Ilorin, P.M.B. 1515, Ilorin, Nigeria
[2]Department of Civil Engineering, Federal Polytechnic Ede, Nigeria
[3]Department of Water Resources and Environmental Engineering, University of Ilorin, Nigeria
[4]Department of Chemical Engineering, University of Ilorin, Nigeria
[5]Department of Industrial Design, Federal University of Technology Akure, Nigeria

*Correspondence: olatunjiaa@gmail.com

SUBMITTED: 10 August 2024; REVISED: 17 September 2024; ACCEPTED: 21 September 2024

ABSTRACT: Wastewater from mining-related activities contains toxic elements that require remediation, and most available wastewater filters have inconsistent flow rates and removal efficiency due to their thickness. This study, therefore, examined the effect of height and size on the flow rate and removal efficiency of a clay composite filter for wastewater remediation. The developed clay filter and its composites were characterized using various techniques such as X-ray fluorescence (XRF), X-ray diffraction (XRD), scanning electron microscopy (SEM), and Fourier transform infrared spectroscopy (FTIR). The XRF analysis showed that the clay contained 91.38% major minerals, including iron oxide (Fe2O3), aluminum oxide (Al2O3), and silica (SiO2), which could enhance the filtration process. Additionally, FTIR revealed that both the clay and the filter are rich in functional groups, including kaolinite and illite, which could promote the filtration process. Further analysis showed that the filters had an average adsorption rate of 87.32%, an average flow rate of 0.891 L/hr, and an average removal efficiency of 99.6%. An increase in the height of a small-diameter filter resulted in a 0.21% increase in removal efficiency, while for larger diameters, the removal efficiency decreased by 0.11%. Conversely, increasing the diameter of a short filter increased the efficiency by 0.25%, while for taller filters, the removal efficiency decreased by 0.07%. Therefore, this work demonstrated that both height and diameter have noticeable effects on flow rate: as height increases, flow rate decreases, and as diameter increases, flow rate increases. The filter's efficiency is somewhat affected by both height and diameter, with a small increase in efficiency noted at greater heights and a slight decrease in efficiency noted at larger diameters.

KEYWORDS: Clay ceramic filter; wastewater remediation; flow rate; removal efficiency; gold mine site

1. Introduction

Global sustainable development, particularly concerning the water environment, relies heavily on environmental conservation. In the face of water scarcity, it is essential not only to safeguard our water resources but also to consider reusing wastewater [1]. The declining quality of many freshwater supplies is a significant environmental concern that has garnered global attention due to its potential negative impacts on both ecosystems and human health [2, 3]. Wastewater containing heavy metals must be treated before being discharged into any receiving water bodies to mitigate its environmental impact [4].

Heavy metals are naturally redistributed throughout the environment through geological and biological cycles, and their exposure to minerals can result in varying concentrations. However, they become harmful to humans once they exceed a certain threshold [5]. According to Tehna et al. [6], Pahimi et al. [7], Fashola et al. [8], and others, waste materials from gold extraction are a major source of heavy metals in water due to the chemical compounds used in gold separation and the operation of excavation machinery. This issue has received international attention because mining-related contamination of water by toxic elements poses serious health risks [9].

Clay is abundant in most parts of the world, moldable, and when fired in a kiln, undergoes a chemical transformation that results in a strong, porous material resistant to deterioration in water [10]. Naturally occurring clay minerals containing alumina, silica, or ferrous metals act as effective oxidants and adsorbents for purifying contaminated water [11]. However, Shivaraju et al. [12] pointed out that despite their widespread availability and use in various water treatment applications, naturally occurring clay minerals have drawbacks, such as low permeability and permanent porosity. To address these issues, it is ideal to convert amorphous clay into a stable, porous ceramic matrix, integrated with active agents and composites. Embedding active chemicals like TiO_2, Ag, Fe, and Cu into the ceramic matrix enhances catalytic oxidation and disinfection during water treatment [12].

Globally, about 1.89 billion tonnes of sugarcane are produced annually. Brazil is the world's largest producer, with an output of 768.7 million tonnes per year, while Nigeria produces around 1.34 million tonnes [13]. The large quantity of bagasse, an agricultural waste left over after sucrose is extracted from sugarcane, presents challenges for treatment and disposal. Utilizing agricultural waste as adsorbents is a practical application of the circular economy and waste beneficiation concepts. Bagasse-based adsorbents are not only more abundant and environmentally friendly than traditional adsorbents like activated carbon, but they are also more affordable [14]. A review shows that bagasse-based adsorbents are highly effective at removing heavy metals from wastewater [15]. Manganese (Mn^{2+}), cadmium (Cd^{2+}), lead (Pb^{2+}), phenol [16], and Cd^{2+} [17] have all been eliminated using sugarcane bagasse [18, 19].

Agricultural wastes such as sugarcane baggase are easily accessible and frequently cause problems with trash disposal. Their application as adsorbents employs the concept of waste beneficiation and circular economy into practice. In addition to their abundance and environmental friendliness, agricultural by-product-derived adsorbents are more cost-effective than traditional adsorbents like activated carbon. Aluminum oxide is an excellent ceramic oxide with a wide range of significant uses in the production of catalysts and adsorbents [20]. It has been applied to eliminate phenol [21] and Cd and Pb [22]. Titanium dioxide nanoparticles have

been used to purify wastewater, and they have shown to function more effectively and quickly [23]. Photocatalyst TiO_2 is becoming more and more popular as an efficient waste water treatment technique [24]. It can be used to treat wastewater because of its high photocatalytic activity, photostability, affordability, and chemical and biological stability [25]. Around the world, clay-based ceramic materials have been utilized to store and cleanse water at points of use [26]. Although there have been a few recent local studies [27–30, 10] that use clay ceramic filters for different wastewater remediation methods, there hasn't been a comprehensive study to look into the impact of clay filter height and size. The primary goal of this study is to determine the effect of height and sizes of clay composite filter on their removal efficiency for wastewater remediation.

2. Materials and Methods

2.1. Materials.

Clay, sugarcane bagasse, aluminum oxide, and titanium dioxide were combined to develop a clay composite filter for gold mining wastewater treatment. The clay sample was obtained from a location near Fountain University, along Abere Road, Osogbo, Osun State, Nigeria, with a latitude of 7.751837 and longitude of 4.532156 (7°45'06.6"N and 4°31'55.8"E) at an elevation of 302.195 meters. The sugarcane bagasse (SCB) was sourced from Sabo, Osogbo, Osun State, Nigeria, with coordinates of 7.782671 latitude and 4.541814 longitude (7°46'57.6"N and 4°32'30.5"E) at an elevation of 302.195 meters. The active agents used were aluminum oxide (Al_2O_3) and titanium dioxide (TiO_2). The gold mining wastewater was collected from a mining site along Muroko Road, Ilesa, Osun State, Nigeria, with a latitude of 7.639550 and longitude of 4.758804 (7°38'22.38"N and 4°45'31.69"E) at an elevation of 384.406 meters. For this study, a clay-to-SCB ratio of 40:60% by volume and an Al_2O_3-to-TiO_2 ratio of 1:4 by weight were selected.

2.2. X-Ray fluorescence and fourier transmission infrared spectroscopy.

An X-ray fluorescence (XRF) analysis was conducted using Phillips PW-1800 equipment to determine the chemical composition of the clay and SCB samples, identifying major and trace elements. XRF operates by analyzing the behavior of atoms when exposed to radiation. The materials were first crushed into pellets smaller than 75 microns and placed in sample holders for analysis [31]. The surface functional groups of the clay and filter were examined using Fourier transform infrared spectroscopy (FTIR) (Shimadzu FTIR 8400S, Japan).

2.3. Filter production.

The ceramic flat filter was developed at a laboratory scale test unit at the Industrial Design Department Studio of the Federal University of Technology Akure, Nigeria. The clay sample and SCB were pulverized into small grains, approximately 1-inch in size, using a jaw crusher. The materials were then sieved using 150µm and 425µm mesh sizes. Prior to adding the active agents (Al_2O_3 and TiO_2), the combustible SCB material and powdered clay were thoroughly mixed. Water was then added to create an even, homogeneous mixture, which was further kneaded and rolled to ensure optimal material combination, following the mixing procedure outlined by Akosile et al. [27].

As shown in Fig. 1, the clay mixture was pressed into cylindrical filter discs in four different sizes: 1.5 cm in height and 7.62 cm in diameter (S1), 1.5 cm in height and 10.16 cm in diameter (B1), 3 cm in height and 7.62 cm in diameter (S3), and 3 cm in height and 10.16 cm in diameter (B3). Each filter size was produced in triplicate. The molded filter discs were air-dried for 16 days at room temperature to preserve their structural integrity before calcination and to prevent cracking or overheating during the firing process. The preliminary test on the control sample indicated a temperature fusing capacity of 800°C due to the high plasticity of the clay. Each ceramic filter was placed in a kiln and sintered for three hours at 800°C. After firing, the filters were allowed to cool at room temperature. Firing increased the material's density (densification), strength, and durability. The average shrinkage of the filter discs during drying was 11.17%, and after firing, the shrinkage increased to 13.33%. No significant variations in shrinkage were observed since the clay content remained consistent across all filters. The finished ceramic flat filter samples were tested for flow rate, water absorption rate, and heavy metal removal efficiency to evaluate the suitability of the clay materials used.

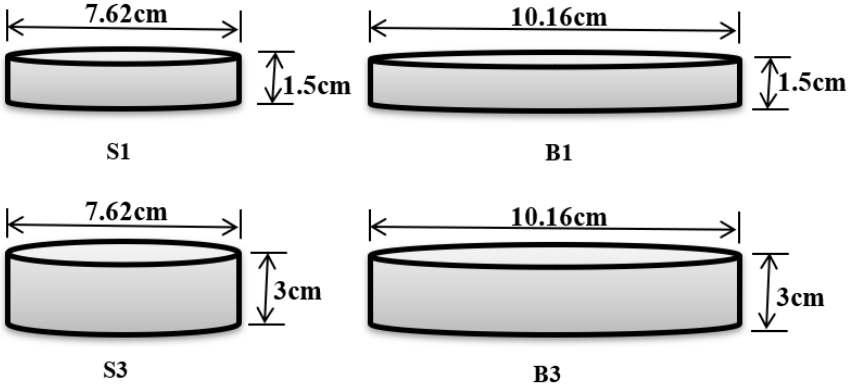

Figure 1. Various sizes of the filter disc S1, B1, S3, B3.

2.4. Scanning electronic microscope and X-Ray diffraction.

Utilizing a TESCAN MIRA3 Scanning Electron Microscope (SEM), the surface morphologies of the filters were examined. The powdered samples were sieved to 0.074 mm and pelletized separately for X-ray diffraction (XRD) analysis. Samples smaller than 2 microns were collected and carefully packed into a 35 mm by 50 mm grid made of aluminum alloy. A wide-angle goniometer (Phillips P.W. 1011) connected to a recorder (PM 8220) was then passed through the sample holder [32].

2.5. Water absorption test.

All the ceramic flat filters were tested for water absorption rates to determine how quickly the filters absorbed water or became saturated. After removal from the kiln, each filter disc was weighed and labeled as the "fired weight." The filters were then soaked in water for 24 hours. After soaking, each sample was removed from the water, lifted, and weighed after a 10-second interval. This process was repeated for each sample to ensure consistency. The filters were dried under constant conditions, and the resulting weight was recorded as the "soaked weight." Water absorption was calculated using the following equation:

$$\boldsymbol{Water\ Absorption}\ \% = \frac{\boldsymbol{soaked\ weight - fired\ weight}}{\boldsymbol{fired\ weight}}\ \boldsymbol{X}\ \mathbf{100}\% \quad (1)$$

2.6. Heavy metal analysis.

The assembled filter discs were suspended from a retort stand, and the wastewater samples were filtered according to standard wastewater examination procedures. The volume of water passing through the filter over a one-hour period was measured to determine the water flow rate. The flow rate was calculated by dividing the volume of filtered water by the flow time. The filtrates were then collected and subjected to a standard digestion process. The digested samples were analyzed using MY2029CQ02 inductively coupled plasma optical emission spectroscopy (ICP-OES) to detect the presence of heavy metals, including arsenic (As), aluminum (Al), gold (Au), copper (Cu), iron (Fe), mercury (Hg), lead (Pb), nickel (Ni), manganese (Mn), and zinc (Zn).

3. Results and Discussion

3.1. X-Ray fluorescence.

According to the chemical composition presented in Table 1, the clay material consists of 4.08% iron oxide (Fe_2O_3), 20.50% aluminum oxide (Al_2O_3), and 66.80% silica (SiO_2). In compliance with ASTM Standard C 618-98, which specifies that the total content of silica, alumina, and iron oxide should be at least 70% for clay materials, the combined percentage of these compounds in the clay is approximately 91.38%. This confirms that the clay used is indeed of high purity. Koopi and Buazar [33] highlighted that Al_2O_3 acts as an adsorbent agent for wastewater treatment and serves as an excellent support for adsorption due to its wide surface area, superior physicochemical properties, high dielectric strength, and thermal stability. These components enhance the filter's adsorption capacity without compromising its structural integrity. For the sugarcane bagasse (SCB), silica and aluminum oxides account for 53.40% and 14.70%, respectively. These components are expected to aid the treatment process and further improve the filter's overall efficiency [11, 34, 35].

Table 1. Chemical composition of clay and SCB.

	SiO_2 (%)	**Al_2O_3 (%)**	**Fe_2O_3 (%)**	**CaO (%)**	**K_2O (%)**	**TiO_2 (%)**	**Na_2O (%)**	**MgO (%)**	**Cl (%)**	**LOI (%)**
Clay	66.80	20.50	4.08	1.70	0.60	0.15	1.65	4.15	0.02	0.35
SCB	53.40	14.70	0.28	1.08	2.02	0.01	0.18	2.20	0.24	0.9

3.2. Fourier transmission infrared spectroscopy analysis.

The peak at 3430–3696 cm^{-1} in the FTIR spectra of the clay material and filter as shown in Figure 2, is attributed to the OH stretching of kaolin and $Al(OH)_3$ used for modification. The methyl C-H peak is located at 2928 cm^{-1}, and the conjugated alkene C=C peak is located at 2353 cm^{-1}. The alkene's C=C is represented by the peaks at 1635 cm^{-1}. The C-O of alcohol and Si-O-Si asymmetric stretching are responsible for the peaks at 1080 and 1103 cm^{-1}, respectively. Al-OH-Al is responsible for the peak in the raw clay at 914 cm^{-1}, whereas Al-O-Si deformation is responsible for the peaks in the clay at 559 and 536 cm^{-1}. The FTIR results for the filter and clay materials agree with those of Olusegun et al. [36]. The raw clay has a high kaolinite content, as indicated by peaks at 3696, 3619, 3430, 1033, 698, and 428 cm^{-1} [37]. Additionally, the peaks at 3619, 3430, 1033 and 536 cm^{-1} suggest the raw is illite-rich while peaks at 3696, 3430, 1635, 1103, 1011, 698, 536 and 467 cm^{-1} are for magnesium-rich chlorite clay as previously reported by Jozanikohan and Abarghooei [37]. These results suggest that the

filter will achieve higher efficiency in wastewater treatment. In summary, the emergence of peaks in the higher spectrum range (3430–3696 cm^{-1}) as indicated by the FTIR spectra may be related to the OH stretching of kaolin and $Al(OH)_3$ utilized for modification. The peaks at 3696, 3619, 3430, 1033, 698, and 428 cm^{-1} indicate that the clay has a high concentration of kaolinite, illite, and magnesium-rich chlorite, all of which are effective heavy metal adsorbents.

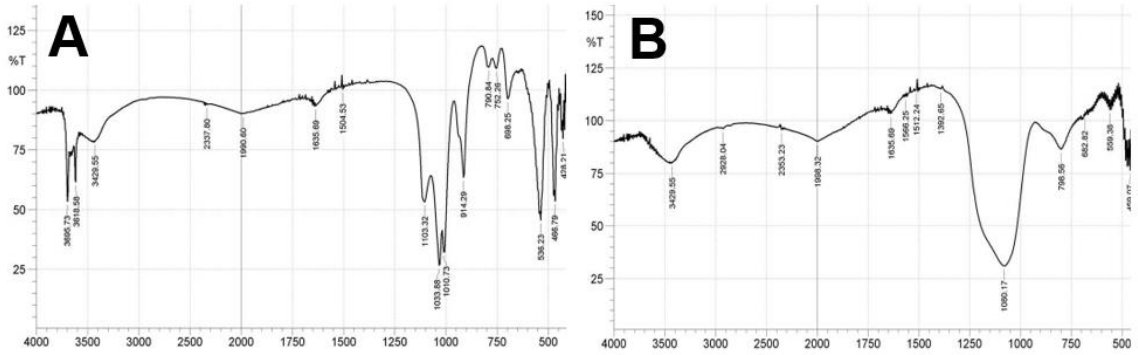

Figure 2. FTIR spectra of raw clay sample (A); filter (B).

3.3. X-Ray diffraction.

The XRD patterns of the filter and active agents are shown in Figure 3. Sharp peaks at 101, 004, 200, 105, 211, 204, and 116 in the active agents' XRD spectra indicate large crystallite sizes that improve wastewater treatment efficiency [38]. The XRD examination of the filter reveals that quartz and kaolinite, both highly effective adsorbents, dominate its crystalline phase components. Additionally, some spectra of dolomite, muscovite, illite, microcline, and calcite were observed, which could further enhance the filter's efficiency in removing heavy metals from wastewater. The effects of the active agent modifications are visible in the filter's peaks, as broad peaks exhibited by alumina indicate its amorphous nature. This observation is consistent with findings reported in the literature [14, 39–40], where the formation of amorphous alumina at a calcination temperature of 900 °C was documented.

3.4. Surface morphology scanning electronic microscope.

The surface morphology of the filter was examined using a scanning electron microscope (SEM), and the resulting image is shown in Figure 4. The SEM image, analyzed using ImageJ software, revealed an average pore area of 72.292 μm² and an average pore length of 66.159 μm. These results suggest that the filter's pores are well-suited for trapping contaminants. The pores were created by the sugarcane bagasse (SCB), which acts as a burnout agent, while the uneven surfaces in the micrograph were caused by Al_2O_3. This finding is consistent with the observations of Rabia et al. [41], who noted that the Al_2O_3 image shows uneven flakes with rough surfaces and small pores between the particles.

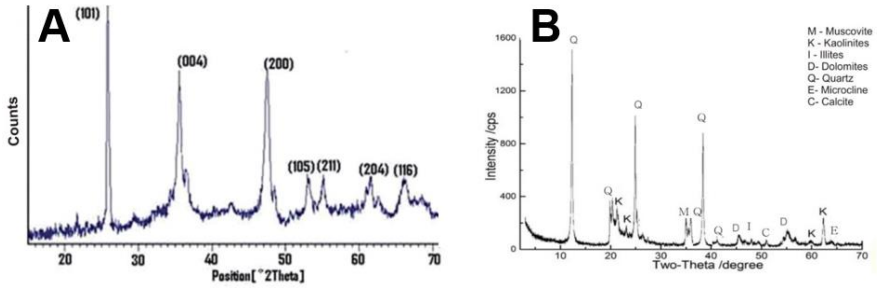

Figure 3. X-ray diffraction patterns of active agents (A); filter (B).

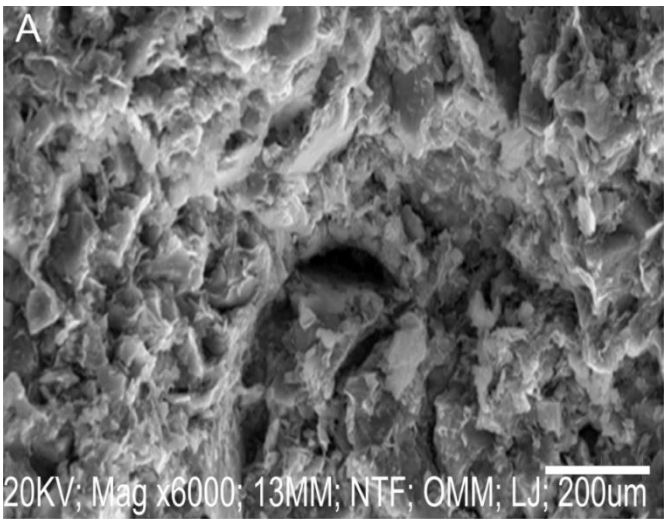

Figure 4. SEM image for the filter.

3.5 Water absorption and flow rate.

Due to the tightly packed nature of clay particles within their structure, clay typically exhibits a low rate of water absorption [27]. This makes the inclusion of pore-formers essential. The water absorption percentage of the filter was measured at 87.32 ± 0.214%, while the average overall flow rate was 0.891 L/hr. Table 2 presents the average flow rates for different filter sizes, along with the effects of height and diameter on flow rates. It was observed that increasing the filter height from 1.5 cm to 3 cm for a 7.62 cm diameter resulted in a 14.54% decrease in flow rate, while the corresponding decrease for a 10.16 cm diameter was 12.77%. This is likely due to the increased travel time for the fluid caused by the greater height. Conversely, an increase in diameter from 7.62 cm to 10.16 cm for a 1.5 cm height led to a 12.1% increase in flow rate, while a 14.42% increase was observed for the 3 cm height with a corresponding diameter. This increase is likely due to the larger number of pores in the filter as the diameter increases. Both height and diameter significantly affect the flow rate: a greater height results in a lower flow rate, while a larger diameter leads to a higher flow rate.

Table 2. Flow rate of varying sizes of filters.

Sample	**S1**	**S3**	**B1**	**B3**
Flow rate (l/h)	0.901	0.770	1.010	0.881
	Effect of height			
	S1 & S3		B1 & B3	
% decrease in flow rate	14.54 %		12.77 %	
	Effect of diameter			
	S1 & B1		S3 & B3	
% increase in flow rate	12.1 %		14.42 %	

3.5 Wastewater result analysis.

Table 3 presents the findings of an investigation into the existence of certain heavy metal ions in the effluent from gold mines, both before and after filtration. Table 3 displays the comparison between these results and the WHO and FEPA standards. The wastewater's pre-filtration results showed that heavy metal ions were present in large quantities, such as As (1.3188 mg/l), Au (1.9024 mg/l), Cu (0.901mg/l), Hg (1.1699 mg/l), Mn (5.875 mg/l), Ni (0.7155 mg/l), Pb (6.934 mg/l), Zn (13.975 mg/l), Fe (194.8684 mg/l) and Al (413.8724 mg/l). The levels of metal ions

found were higher than what the WHO and FEPA considered being acceptable. Therefore, it is essential to remove them from the wastewater prior to releasing the water into the surrounding environment. The study of the filtration process using the developed filter shows that all filters completely eliminate mercury ion from the wastewater as they were below the machine detection level, filter S1 was able to achieve complete removal for gold ions as well, while others reduced the concentration of all ions below the standards.

Table 3. Concentration of metal ions in gold mine wastewater and the standards.

Element	Raw	After filtration				WHO	FEPA
		S1	S3	B1	B3		
Al (mg/l)	413.8724	0.054449	0.028028	0.009359	0.00648	NA	NA
As (mg/l)	1.3188	0.003878	0.000181	0.004052	0.004249	0.5	0.1
Au (mg/l)	1.9024	-0.001158	0.003656	0.007539	0.015824	0.01	NA
Cu (mg/l)	0.901	0.002197	0.000753	0.000232	0.00072	1.0	< 1
Fe (mg/l)	194.8684	0.053111	0.040236	0.021799	0.018139	10	20
Hg (mg/l)	1.1699	-0.002025	-0.00319	-0.00122	-0.00056	0.005	0.05
Mn (mg/l)	5.875	0.037244	0.006883	0.010305	0.004499	0.2 (10)	5
Ni (mg/l)	0.7155	0.025708	0.022884	0.013424	0.018877	0.1 (1)	< 1
Pb (mg/l)	6.934	0.013076	0.007208	0.03385	0.031869	0.1 (1)	< 1
Zn (mg/l)	13.975	0.132587	0.011633	0.017959	0.005991	3.0 (5)	< 1

NA – Not available

3.6 Removal efficiency.

The percentage removal efficiency of the filter was evaluated using the equation 2 and are presented in Table 4.

$$R = \frac{C_0 - C_t}{C_0} \; X \; 100\% \qquad (2)$$

where R is the removal percentage of each parameter (%), C_0 and C_t are the initial and final concentrations of each parameter (mg/l).

The percentage removal efficiency ranges from the minimum 96.407 % to the maximum of 100 %. Every filter was able to remove mercury with 100% effectiveness. Additionally, filter S1 was successful in eliminating all gold ions. With the exception of nickel, which had results of 96.407%, 96.702 %, 98.124 %, and 97.362 % for S1, S3, B1, and B3, respectively, all filters were able to achieve above 99 %.

Table 4. Percentage removal efficiency of the filters.

Element	S1	S3	B1	B3
	Removal efficiency (%)			
Al	99.987	99.993	99.998	99.998
As	99.706	99.986	99.693	99.678
Au	100	99.808	99.604	99.168
Cu	99.756	99.916	99.974	99.920
Fe	99.973	99.979	99.989	99.991
Hg	100	100	100	100
Mn	99.366	99.883	99.825	99.923
Ni	96.407	96.802	98.124	97.362
Pb	99.811	99.896	99.512	99.540
Zn	99.051	99.917	99.871	99.957

The overall efficiency of each filter are presented in Fig. 5 with filter B1 having highest efficiency rate of 99.66 % while filter S1 had the least efficiency at 99.41 %. It was observed that all the filters achieved above 99%, an indication of very effective filters. The addition of active elements (Al_2O_3 and TiO_2) may have contributed to these greater efficiencies, while the average efficiency of filters manufactured without them was 89.92%.

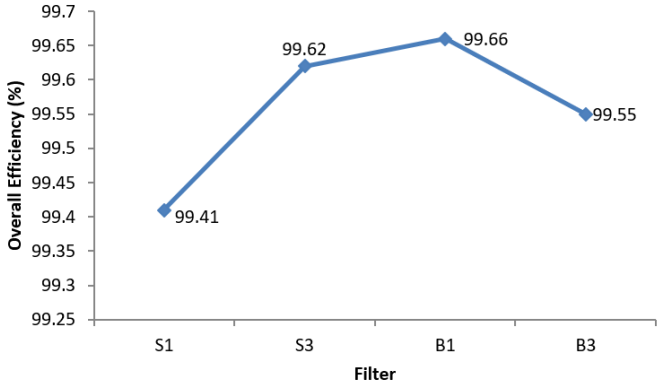

Figure 5. Overall percentage removal efficiency of all filters.

3.7 Effect of height and diameter on the efficiency of the filter.

The impact of diameter and height on the filters' efficiency is seen in Figure 6. When filters S1 and S3, which have the same diameter but different heights, are compared, S3 appears to be more efficient (99.62%) than S1 (99.41%) by just 0.21%. This could be because the height increase causes a longer contact time during filtration. Conversely, B1 and B3 exhibit the reverse trend, with their respective efficiency dropping from 96.66% to 99.55%, or a 0.11 percent reduction. This could potentially be attributed to the filter's wider pores increasing in number.

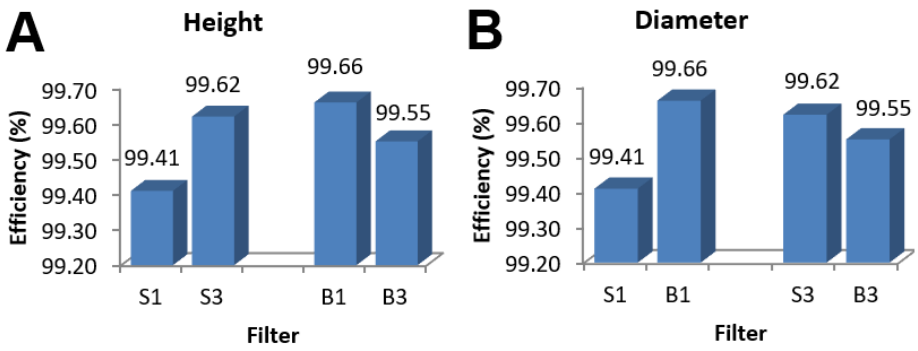

Figure 6. Filter efficiency based on height (A); diameter (B).

On the other hand, it was also examined how changing the diameter affected the filters' efficiency, as seen in Fig. 6B. When filter S1 and B1, which have the same height but different diameters, are compared, the figure indicates a 0.25 % increase in efficiency, which may be explained by the increased adsorption site that the larger filter's diameter creates. Nonetheless, there was a 0.07% decrease in efficiency when comparing the filters S3 and B3. Even while the decrease in efficiency might not seem like much, it could be caused by the active agents contained in the filter extending due to the rise in height, which also applies to height analysis. In conclusion, both height and diameter have very little impact on the filter's effectiveness since, while variances are acknowledged, little increase in efficiency is noted at greater heights and a slight decrease in efficiency is noted at bigger diameters.

4. Conclusions

A composite wastewater filter was developed and put through a number of tests, all of which verified that the filter captured heavy metal ions—a sign that adsorption had occurred. Based on the analysis and results, it can be said that the filter's high adsorption rate of 87.32% helps to increase its flow rate. The flow rate increases by 13.26% on average when the filter's diameter increases, but it decreases by 13.66% when the filter's height increases. The active elements significantly increased the filters' performance, which resulted in an average removal efficiency of 99.6%. The filter's efficiency is somewhat affected by both height and diameter; a small increase in efficiency is noted at higher heights, and a slight decrease in efficiency is noted at bigger diameters. Even though all of the efficiency changes appear to be very slight—they are all above 99%—they nonetheless represent changes that should be documented even though they might not be felt in practical applications. The authors propose that slightly increasing the diameter while keeping the height the same will result in the best performance, as evidenced by the total efficiency.

Acknowledgments

The assistance of Associate Professor L. Azeez of the pure and applied chemistry department, osun state university, Osogbo, Nigeria is highly appreciated. Likewise, the effort of Mr. Oke of the studio of industrial design department, federal university of technology, Akure, Nigeria is appreciated for the laboratory works.

Author Contribution

A. A. Olatunji: Conceptualization, Methodology, Data Collection, Data Analysis, Writing – original draft, editing, Funding. **A. M. Ayanshola:** Supervision, Methodology, Writing – review & editing. **M. A. Ajala:** Supervision, Data Analysis. **E. Erhuanga:** Methodology, Data Analysis.

Competing Interest

All authors have no competing interest to declare.

References

[1] Hu, Z.; Yan, S.; Li, X.; Yao, L.; Zhifeng, L. (2019). Evaluating the oil production and wastewater treatment efficiency by an extended two-stage network structure model with feedback variables. *Journal of Environmental Management*, *251*, 109578. https://doi.org/10.1016/j.jenvman.2019.109578.

[2] Emenike, P.C.; Omole, D.O.; Ngene, B.U.; Tenebe, I.T. (2016). Potentiality of agricultural adsorbent for the sequestering of metal ions from wastewater. *Global Journal of Environmental Science and Management*, *2*, 411e442. https://doi.org/10.22034/gjesm.2016.02.04.010.

[3] Hanna, W.; Wan, M.; Nizam, K.; Maulud, A.; Shazwani, N.; Sharil, S.; Mundher, Z. (2019). Spatial and temporal risk quotient based river assessment for water resources management. *Environmental Pollution*, *248*, 133e144. https://doi.org/10.1016/j.envpol.2019.02.011.

[4] Abdullah, W.N.A.S.; Tiandee, S.; Lau, W.J.; Aziz, F.; Ismail, A.F. (2019). Potential use of nanofiltration like-forward osmosis membranes for copper ion removal. *Chinese Journal of Chemical Engineering*, *28*(2), 420–428. https://doi.org/10.1016/j.cjche.2019.05.016.

[5] Rakotondrabe, F.; Ngoupayou, J.R.N.; Mfonka, Z.; Rasolomanana, E.H.; Abolo, A.J.N.; Ako, A.A. (2018). Water quality assessment in the bétaré-oya gold mining area (east-cameroon): multivariate statistical analysis approach. *Science of the Total Environment, 610–611*, 831–844. http://doi.org/10.1016/j.scitotenv.2017.08.080.

[6] Tehna, N.; Nguene, F.D.; Etame, J.; Medza Ekodo, J.M.; Noa-Tang, S.; Suh, E.C.; Bilong, P. (2015). Impending pollution of betare oya opencast mining environment (Eastern Cameroon). *Journal of Environmental Science and Engineering B, 4*, 37–46. http://doi.org/10.17265/2162-5263/2015.01.006.

[7] Pahimi, H.; Panda, C.R.; Ngassoum, M.B.; Tchameni, R. (2015). Environmental impacts of mining in the volcano-sedimentary basins of cameroon: case study of artisanal gold mine tailings (Betare Oya, East-Cameroon). *International Journal of Energy and Environmental Engineering, 2*, 5–15.

[8] Fashola, M.O.; Ngole-Jeme, V.M.; Babalola, O.O. (2016). Heavy metal pollution from gold mines: environmental effects and bacterial strategies for resistance. *International Journal of Environmental Research and Public Health, 13*, 1047. http://doi.org/10.3390/ijerph13111047.

[9] Odukoya, A.M.; Olobaniyi, S.B.; Oluseyi, T.O.; Adeyeye, U.A. (2017). Health risk associated with some toxic elements in surface water of Ilesha gold mine sites, Southwest Nigeria. *Environmental Nanotechnology, Monitoring & Management, 8*, 290–296. http://doi.org/10.1016/j.enmm.2017.10.005.

[10] Ajayi, B.A.; Lamidi, Y.D. (2015). Formulation of ceramic water filter composition for the treatment of heavy metals and correction of physiochemical parameters in household water. *Art and Design Review, 3*, 94–100. http://doi.org/10.4236/adr.2015.34013.

[11] Tom, N.K.; Sivan, S.; Giora, R. (2012). Brine wastewater pretreatment using clay minerals and organoclays as flocculants. *Applied Clay Science, 67*, 119–124. https://doi.org/10.1016/j.clay.2012.05.009.

[12] Shivaraju, H.P.; Egumbo, H.; Madhusudan, P.; Anil-Kumar, K.M.; Midhun, G. (2018). Preparation of affordable and multi-functional clay-based ceramic filter matrix for treatment of drinking water. *Environmental Technology*, *40*(13), 1633–1643. https://doi.org/10.1080/09593330.2018.1430853.

[13] List of countries by sugarcane production. (accessed on 14 April 2021) Available online: https://www.atlasbig.com/en-gb/countries-by-sugarcane-production.

[14] Ajala, E.O.; Aliyu, M.O.; Ajala, M.A.; Mamba, G.; Ndana, A.M.; Olatunde, T.S. (2024). Adsorption of lead and chromium ions from electroplating wastewater using plantain stalk modified by amorphous alumina developed from waste cans. *Scientific Reports, 14*, 6055. https://doi.org/10.1038/s41598-024-56183-2.

[15] Velazquez-Jimenez, L.H.; Pavlick, A.; Rangel-Mendez, J.R. (2013). Chemical characterization of raw and treated agave bagasse and its potential as adsorbent of metal cations from water. *Journal of Industrial Crops Production, 43*, 200–206. https://doi.org/10.1016/j.indcrop.2012.06.049.

[16] Sonawane, B.K.; Korake, S.R. (2016). Review on removal of phenol from wastewater using low cost adsorbent. *International Journal of Science, Engineering and Technological Resources, 5*, 2249–2253.

[17] Moubarik, A.; Grimi, N. (2015). Valorization of olive stone and sugarcane bagasse by-products as biosorbents for the removal of cadmium from aqueous solution. *Food Resources International, 73*, 169–175. https://doi.org/10.1016/j.foodres.2014.07.050.

[18] Anastopoulos, I.; Bhatnagar, A.; Hameed, B.H.; Ok, Y.S.; Omirou, M. (2017). A Review on waste-derived adsorbents from sugar industry for pollutant removal in water and wastewater. *Journal of Molecular Liquids, 240*, 179–188. https://doi.org/10.1016/j.molliq.2017.05.063.

[19] Abdelhafez, A.A.; Li, J. (2016). Removal of Pb (II) from aqueous solution by using biochars derived from sugarcane bagasse and orange peel. *Journal of Taiwan Institute of Chemical Engineers*, *61*, 367–375. https://doi.org/10.1016/j.jtice.2016.01.005.

[20] Aluminium Oxide – Al_2O_3. (accessed on 29 March 2023) Available online: https://byjus.com/chemistry/al2o3/.

[21] Safwat, M.S.; Mohamed, N.Y.; Mohamed, N. A.; Meshref-Elawwad, A. (2022). Adsorption of phenol onto aluminum oxide nanoparticles: performance evaluation, mechanism exploration, and principal component analysis (PCA) of thermodynamics. *Adsorption Science & Technology*, 2022. https://doi.org/10.1155/2022/1924117.

[22] Tabesh, S.; Davar, F.; Loghman-Estarki, M.R. (2018). Preparation of γ-Al_2O_3 nanoparticles using modified sol-gel method and its use for the adsorption of lead and cadmium ions. *Journal of Alloys and Compounds*, *730*, 441–449. https://doi.org/10.1016/j.jallcom.2017.09.246.

[23] Azeez, L.; Lateef, A.; Adebisi, S.A.; Oyedeji, A.O. (2018). Novel biosynthesized silver nanoparticles from cobweb as adsorbent for rhodamine b: equilibrium isotherm, kinetic and thermodynamic studies. *Applied Water Science*, *8*(1), 32. https://doi.org/10.1007/s13201-018-0676-z.

[24] Yaqoob, S.; Ullah, F.; Mehmood, S.; Mahmood, T.; Ullah, M.; Khattak, A.; Zeb, M.A. (2018). Effect of waste water treated with TiO_2 nanoparticles on early seedling growth of *Zea mays*. *Journal of Water Reuse and Desalination*, *8*(3), 424–431. https://doi.org/10.2166/wrd.2017.163.

[25] Emamverdian, A.; Ding, Y.; Mokhberdoran, F.; Ahmad, Z.; Xie, Y. (2021). The investigation of tio_2 nps effect as a wastewater treatment to mitigate cd negative impact on bamboo growth. *Sustainability*, *13*, 3200. https://doi.org/10.3390/su13063200.

[26] Ajibade, F.O.; Akosile, S.I.; Oluwatuyi, O.E.; Ajibade, T.F.; Lasisi, K.H.; Adewumi, J.R.; Babatola, J.O.; Oguntuase, A.M. (2019). Bacteria removal efficiency data and properties of Nigerian clay used as a household ceramic water filter. *Results in Engineering*, *2*, 100011. https://doi.org/10.1016/j.rineng.2019.100011.

[27] Akosile, S.I.; Ajibade, F.O.; Lasisi, K.H.; Ajibade, T.F.; Adewumi, J.R.; Babatola, J.O.; Oguntuase, A.M. (2020). Performance evaluation of locally produced ceramic filters for household water treatment in Nigeria. *Scientific African*, *7*, e00218. https://doi.org/10.1016/j.sciaf.2019.e00218.

[28] Ojuri, O.O.; Oluwatuyi, O.E. (2018). Compacted sawdust ash-lime stabilised soil-based hydraulic barriers for waste containment. *Proceedngs of the Institution of Civil Engineers - Waste Resources Management*, *171*, 52–60. https://doi.org/10.1680/jwarm.17.00037.

[29] Agbo, S.C.; Ekpunobi, E.U.; Onu, C.C.; Akpomie, K.G. (2017). Development of ceramic filter candle from nsu (kaolinite clay) for household water treatment. *International Journal of Multidiscipline Science and Engineering*, *6*(10), 18–23.

[30] Nnaji, C.C.; Afangideh, B.C.; Ezeh, C. (2016). Performance evaluation of clay-sawdust composite filter for point of use water treatment. *Nigerian Journal of Technology (NIJOTECH)*, *35*(4), 949–956. http://dx.doi.org/10.4314/njt.v35i4.33.

[31] Margui, E.; Queralt, I.; Grieken, R.V. (2016). Sample preparation for X-ray fluorescence analysis. *Encyclopedia of Analytical Chemistry*, 1–25. https://doi.org/10.1002/9780470027318.a6806.pub4.

[32] Bunaciu, A.A.; Udristioiu, E.G.; Aboul-Enein, H.Y. (2015). X-ray diffraction: Instrumentation and applications. *Critical Reviews in Analytical Chemistry*, *45*(4), 289–299. https://doi.org/10.1080/10408347.2014.949616.

[33] Koopi, H.; Buazar, F. (2019). A novel one-pot biosynthesis of pure alpha aluminium oxide nanoparticles using the macroalgae *Sargassum ilicifolium*: A green marine approach. *Ceramics International*, *44*, 8940–8945. https://doi.org/10.1016/j.ceramint.2018.02.091.

[34] Ajayi, B.A.; Lamidi, Y.D.; Owoeye, S.S. (2013). Possibility of using glass-snail shell for industrial waste water treatment. *International Research Journal, 3,* 8-11.

[35] Wuana, R.A.; Okieimen, F.E.; Imborvungu, J.A. (2010). Removal of heavy metals from a contaminated soil using organic chelating acids. *International Journal of Environmental Science and Technology*, *7*, 485–496. https://doi.org/10.1007/BF03326158.

[36] Olusegun, S.J.; Lima, L.F.; Mohallem, N.D.S. (2018). Enhancement of adsorption capacity of clay through spray drying and surface modification process for wastewater treatment. *Chemical Engineering Journal*, *334*, 1719–1728. https://doi.org/10.1016/j.cej.2017.11.084.

[37] Jozanikohan, G.; Abarghooei, M.N. (2022). The fourier transform infrared spectroscopy (FTIR) analysis for the clay mineralogy studies in a clastic reservoir. *Journal of Petroleum Exploration and Production Technology*, *12*, 2093–2106. https://doi.org/10.1007/s13202-021-01449-y.

[38] Raja, P.B.; Munusamy, K.R.; Perumal, V.; Mohamad Ibrahim, M.N. (2022). Characterization of nanomaterial used in nanobioremediation, in Nano-Bioremediation: Fundamentals and Applications. *Micro and Nano Technologies*, *2022*, 57–83. https://doi.org/10.1016/B978-0-12-823962-9.00037-4.

[39] Yu H.; Wang M.; Zhou J.; Yuan B.; Luo J.; Wu W.; Chen Z.; Yu R. (2020). Microreactor-assisted synthesis of α-alumina nanoparticles. *Ceramics International*, *46*(9), 13272–13281. https://doi.org/10.1016/j.ceramint.2020.02.105.

[40] Xiang H.; Wang Z.; Yin Q.; Wang L.; Zhang L.; Wang H.; Xu H.; Zhang R.; Lu H. (2019). Effect of process factors on properties of high dispersion spherical α-Al2O3 particles prepared by hydrothermal method. *Ceramics International*, *45*(17), 22007–22014. https://doi.org/10.1016/j.ceramint.2019.07.215.

[41] Rabia, A.R.; Ibrahim, A.H.; Zulkepli, N.N. (2018). Activated alumina preparation and characterization: The review on recent advancement. *E3S Web Conferences*, *34*, 1–8. https://doi.org/10.1051/e3sconf/20183402049.